AFRL-RX-WP-TP-2012-0372

FORMATION OF EQUIAXED ALPHA AND TITANIUM NITRIDE PRECIPITATES IN SPARK PLASMA SINTERED TiB/Ti-6Al-4V COMPOSITES (PREPRINT)

P.Nandwana and R. Banerjee
University of North Texas

J.Y Hwang
Korea Institute of Science and Technology

M.Y. Koo and S.H. Hong
Korea Advanced Institute of Science and Technology

J. Tiley
Metals Branch
Structural Materials Division

August 2012
Interim

AIR FORCE RESEARCH LABORATORY
MATERIALS AND MANUFACTURING DIRECTORATE
WRIGHT-PATTERSON AIR FORCE BASE, OH 45433-7750
AIR FORCE MATERIEL COMMAND
UNITED STATES AIR FORCE

REPORT DOCUMENTATION PAGE

Form Approved
OMB No. 0704-0188

1. REPORT DATE *(DD-MM-YY)*	2. REPORT TYPE	3. DATES COVERED *(From - To)*
August 2012	Technical Paper	1 July 2012 – 1 August 2012

4. TITLE AND SUBTITLE

FORMATION OF EQUIAXED ALPHA AND TITANIUM NITRIDE PRECIPITATES IN SPARK PLASMA SINTERED TiB/Ti-6Al-4V COMPOSITES (PREPRINT)

5a. CONTRACT NUMBER
FA8650-08-C-5226

5b. GRANT NUMBER

5c. PROGRAM ELEMENT NUMBER
62102F

6. AUTHOR(S)

P.Nandwana and R. Banerjee (University of North Texas)
J.Y Hwang (Korea Institute of Science and Technology)
M.Y. Koo and S.H. Hong (Korea Advanced Institute of Science and Technology)
J. Tiley (AFRL/RXCM)

5d. PROJECT NUMBER
4347

5e. TASK NUMBER

5f. WORK UNIT NUMBER
LM114100

7. PERFORMING ORGANIZATION NAME(S) AND ADDRESS(ES)

University of North Texas
Corner of Avenue C Chestnut
Denton, TX 76203

8. PERFORMING ORGANIZATION REPORT NUMBER

9. SPONSORING/MONITORING AGENCY NAME(S) AND ADDRESS(ES)

Air Force Research Laboratory
Materials and Manufacturing Directorate
Wright-Patterson Air Force Base, OH 45433-7750
Air Force Materiel Command
United States Air Force

10. SPONSORING/MONITORING AGENCY ACRONYM(S)
AFRL/RXCM

11. SPONSORING/MONITORING AGENCY REPORT NUMBER(S)
AFRL-RX-WP-TP-2012-0372

12. DISTRIBUTION/AVAILABILITY STATEMENT

Approved for public release; distribution unlimited. Preprint to be submitted to Materials Letters

13. SUPPLEMENTARY NOTES

The U.S. Government is joint author of this work and has the right to use, modify, reproduce, release, perform, display, or disclose the work. PA Case Number and clearance date: 88ABW-2012-2627, 7 May 2012. This document contains color.

14. ABSTRACT

Spark plasma sintered TiB/Ti-6Al-4V composites have been characterized using scanning electron microscopy (SEM), electron backscattered diffraction (EBSD) and transmission electron microscopy (TEM). As-SPS processed composites exhibit a more refined distribution of equiaxed α precipitates as compared to arc-melted composites containing similar volume fraction of TiB precipitates. Additionally, SPS processed composites also show a highly refined distribution of TiN precipitates, as revealed by TEM studies.

15. SUBJECT TERMS

Ti-6Al-4V; TiB; TiN; Spark Plasma Sintering; Composite; α/β phase

16. SECURITY CLASSIFICATION OF:			17. LIMITATION OF ABSTRACT:	NUMBER OF PAGES	19a. NAME OF RESPONSIBLE PERSON (Monitor)
a. REPORT	b. ABSTRACT	c. THIS PAGE			Jaimie Tiley
Unclassified	Unclassified	Unclassified	SAR	10	19b. TELEPHONE NUMBER *(Include Area Code)* N/A

Formation of equiaxed alpha and titanium nitride precipitates in spark plasma sintered TiB/Ti-6Al-4V composites

P. Nandwana[1], J.Y. Hwang[2], M. Y. Koo[3], J. Tiley[4], S. H. Hong[3], and R. Banerjee[1]

[1] Department of Materials Science and Engineering, University of North Texas, Denton, TX 76203, USA

[2] Korea Institute of Science and Technology, Seoul, 136-791, Korea

[3] Korea Advanced Institute of Science and Technology, Daejeon, 305-701, Korea

[4]Materials and Manufacturing Directorate, Air Force Research Laboratory, Dayton, OH 45433, USA

Abstract

Spark plasma sintered TiB/Ti-6Al-4V composites have been characterized using scanning electron microscopy (SEM), electron backscattered diffraction (EBSD) and transmission electron microscopy (TEM). As-SPS processed composites exhibit a more refined distribution of equiaxed α precipitates as compared to arc-melted composites containing similar volume fraction of TiB precipitates. Additionally, SPS processed composites also show a highly refined distribution of TiN precipitates, as revealed by TEM studies.

Keywords: Ti-6Al-4V; TiB; TiN; Spark Plasma Sintering; Composite; α/β phase

Introduction

Trace amounts of boron addition to conventional titanium alloys has been found to have a considerable impact on the microstructure and the properties [1]. These composites offer improved mechanical properties by combining high strength and stiffness of TiB with the toughness of the Ti alloy matrix [2]. Several researchers have reported that addition of boron also results in refinement of prior β grain size as well as reduction in the α grain size as TiB acts as pinning sites hence restricting grain growth [3-5]. Traditionally, powder metallurgy and common casting techniques were used to fabricate titanium matrix composites. In recent years, novel in situ processing techniques like spark plasma sintering (SPS), self-propagating high temperature synthesis (SHS) and laser engineered net shaping (LENS^{TM}) etc. have aroused interest as they offer the advantage of a homogenous distribution of borides in the matrix [6]. Commercially used α/β titanium alloys typically are subjected to thermo-mechanical processing to attain the desired microstructure relevant to the application. TiB precipitates have been found to influence the nucleation of α phase by acting as heterogeneous nucleation sites in addition to the usual prior β grain boundaries. It has also been reported in the literature that α nucleating from the TiB obeys an orientation relationship $(001)_{TiB}//(0001)_{\alpha}$, $[010]_{TiB}//[11\text{-}20]_{\alpha}$ [7]. The present paper discusses the effect of boron addition on the size and morphology of α in TiB/Ti-6Al-4Vcomposites fabricated using the SPS process and compares it with conventional arc-melted samples.

Experimental

TiB_2 powder with a mean particle size of ~3μm was mixed with pre- alloyed Ti-6Al-4V powder of mean particle size ~30μm. Additional Ti powder was added to allow for reaction with TiB_2 to form TiB in order to maintain the composition of the base alloy. Mechanical alloying was carried out using planetary ball milling under nitrogen atmosphere and subsequently the powders were spark plasma sintered at a temperature of 1373K for 5 minutes employing a pressure of 50MPa under a vacuum of 10^{-3}torr. For comparison purposes, Ti-6Al-4V/TiB composites with different volume fractions of TiB were also fabricated via arc-melting of pre-alloyed Ti-6Al-4V and TiB_2 powders. These arc-melted samples were solutionized at 1373K for 30 minutes followed by furnace cooling to allow for complete dissolution of α during the β solutionizing process. The specimens were cut by wire electro discharge machining (EDM) and subsequently mechanically polished to a mirror finish using 0.05μm colloidal silica to minimize surface deformation. The microstructure was investigated using a FEI NOVA Nano SEM instrument. Electron backscatter diffraction (EBSD) studies were also carried out to determine the presence of orientation relationships between TiB and α phase, if any. TEM investigations were carried out on conventional 3mm diameter disc samples. The TEM samples were analyzed in a FEI Tecnai F20 microscope operating at 200kV.

Results and discussion

The overall microstructure of the SPS processed TiB/Ti-6Al-4V composite is shown in the backscatter SEM images, Figs. 1(a) and (b). The microstructure consists of acicular, needle-like TiB precipitates (dark contrast) dispersed in an α+β matrix with α displaying an equiaxed (or globular) morphology. The higher magnification image in Fig. 1(b) shows the presence of an additional unknown fine scale spherical precipitate, homogenously distributed in the matrix. The TiB precipitates have an acicular morphology with a length of about 5-10μm and widths ranging from 0.5-2μm. The size range of the second reinforcement phase, exhibiting a spherical morphology, is 100-300nm. The area fraction of the borides was determined using basic two-dimensional image analysis techniques and was found to be ~1% and for simplicity this value was assumed to be an approximate measure of the boride volume fraction. This sample will henceforth be referred to Ti64-1TiB. Similar nomenclature will be adopted for other samples as well. Fig. 1(c) and (d) show the microstructure of the arc melted composites. The area fraction of the borides was found to be 1% and 2% respectively. The backscatter SEM images clearly show that the distribution of borides in the SPS processed Ti64-1TiB composite is more homogenous compared to the arc-melted composites where TiB appears to be decorating the prior β grain boundaries. The absence of TiB along prior β grain boundaries in the SPS processed sample is definitely an advantage of this type of processing, obviating the deleterious effects of β grain boundaries decorated by hard non-deformable TiB precipitates. The microstructural difference between the two processing routes arises from the fact that while arc-melting results in the entire system first melting and then solidifying, SPS process is primarily based on solid-state processing involving localized melting in some cases but does not involve homogeneous solidification of a liquid.

A common feature to be observed for all samples is that α in the immediate vicinity of TiB appears to adopt an equiaxed morphology compared to α further away from TiB precipitates which exhibits a more lath-like morphology. This effect is predominantly seen in case of the arc-melted Ti64-1TiB and Ti64-2TiB composites. These observations clearly indicate that the TiB precipitates influence the morphology of α phase and consequently it is important to investigate the possible existence of orientation relationships between these two phases as discussed subsequently in this paper. The backscatter SEM micrographs clearly reveal that the Ti64-1TiB composite, processed by SPS, has much finer scale α as compared to the arc-melted samples. The same level of refinement may be achieved by thermo-mechanical processing of the same microstructure in the α+β regime but SPS offers the novel advantage that the refined equiaxed α is obtained during sintering at a temperature above the β transus temperature. Therefore, SPS processing results in fine scale equiaxed α formation in TiB/Ti-6Al-4V composites without the costs and time associated with an additional thermo-mechanical processing step post synthesis, as required for arc melted composites. From the SEM micrographs it is evident that SPS processing allows for a higher fraction of refined equiaxed α, for much lower volume fractions of TiB, potentially leading to a superior balance of material properties as compared to composites with higher TiB volume fractions.

The results of crystallographic EBSD-orientation imaging microscopy (OIM) investigations of SPS processed Ti64-1TiB composite have been summarized in Fig. 2 with the inverse pole figure map of the overall microstructure shown in Fig. 2(a). Figs. 2(b) and (c) show specific selected TiB and α precipitates, along with their corresponding pole figure maps. The pole figures clearly reveal two distinct orientation relationships between the TiB and α, which are $(001)_{TiB}//(0001)_{\alpha}$, $[010]_{TiB}//[11\text{-}20]_{\alpha}$ and $(101)_{TiB}//(01\text{-}10)_{\alpha}$, $[010]_{TiB}//[11\text{-}20]_{\alpha}$ and will be subsequently referred to as OR1 and OR2 respectively. In recent studies on β titanium alloys the existence of multiple orientation relationships between α and TiB have been reported [8, 9]. OR1 is the most commonly observed orientation relationship in TiB/Ti-6Al-4V composites but OR2 has not been reported for this system yet. Fig. 2(d) shows the inverse pole figure map from a different region of the SPS processed sample and a specific combination of a TiB and a α precipitate together with their corresponding pole figures are shown in Fig. 2(e). The OR2 relationship between the TiB and the α precipitate is evident in this case. Similar observations of ORs between TiB and α in many different regions of the sample, clearly indicate that the TiB precipitates act as nucleation sites for α. Based on these observations it can be speculated that the development of an orientation relationship between TiB and α could potentially result in the loss of the classical Burgers orientation relationship between the α precipitates and the β matrix. Consequently, the morphology of α precipitates, that is closely associated with the α/β orientation relationship, can change, leading to the formation of more equiaxed α nucleating from the TiB.

Fig. 3(a) shows a bright field TEM image of the SPS processed Ti64-1TiB composite with a diffracting β pocket (dark contrast) between α precipitates. Fig. 3(b) shows a TiB precipitate, with a high density of faulting within the boride aligned parallel to the $(100)_{TiB}$ planes and Fig. 3(c) provides a clearer view of the high fault density within the boride and the electron diffraction pattern shown as an inset can be consistently indexed as the [001] zone axis of the orthorhombic B27 structure of TiB. The mechanism of

formation of facets in these TiB precipitates and faulting parallel to the the (100) planes, has been widely discussed in the literature [10, 11]. Fig. 3(d) shows a bright field TEM image of one of the unidentified precipitates in the SPS processed composite. Selected area diffraction analysis was carried out to determine the crystal structure of this unknown phase. These precipitates were found to have a face-centered cubic (*fcc*) crystal structure with a lattice parameter of a=0.42nm. Figs. 3(e) and (f) show converged beam micro-diffraction patterns of the unknown precipitate along the [001] and [113] zone axes respectively. EDS and EELS revealed the presence of nitrogen peaks in these precipitates hence they are likely to be TiN. This argument is augmented by the fact that since the powders were mechanically alloyed in nitrogen atmosphere prior to sintering; it is highly likely that Ti reacts with the residual nitrogen to form TiN. These homogeneously distributed TiN precipitates are likely to enhance the strength of this composite via precipitation hardening.

Conclusions

Based on EBSD and TEM studies it can be concluded that spark plasma sintering is a novel processing technique to obtain TiB/Ti-6Al-4V composites with fine scale equiaxed alpha with small boron additions unlike arc melting which requires much higher boride volume fraction to achieve the same degree of refining. TiB has been found to act as nucleation sites for α as evident from the orientation relationships between the two phases. The orientation relationships between these two phases are $(001)_{TiB}//(0001)_{\alpha}$, $[010]_{TiB}//[11\text{-}20]_{\alpha}$ and $(101)_{TiB}//(01\text{-}10)_{\alpha}$, $[010]_{TiB}//[11\text{-}20]_{\alpha}$ where the latter orientation relationship has been reported for the first time for this system. Additionally, a highly refined and homogeneous distribution of TiN precipitates was also observed within the matrix, possibly resulting from the nitrogen gas involved during mechanical alloying process prior to sintering.

Acknowledgements

This work has been supported in part by the National Space Lab program (N01090333) through the Korea Science and Engineering Foundation funded by the Ministry of Educaion, Science and Technology, and Defense Acqisition Program Administration and Agency for Defense Development under Basic Research program (UD080009GD) as well as the ISES contract awarded to the University of North Texas by the U.S. Air Force Research Laboratory, AFRL contract number FA8650-08-C-5226. The authors also gratefully acknowledge the Center for Advanced Research and Technology (CART) at the University of North Texas.

References

1. M.J. Bermingham, S.D. McDonald, K. Nogita, D.H. St. John, M.S. Dargusch; Scripta Mater 2008 538-541.
2. A. Genç, R. Banerjee, D. Hll, H.L. Fraser; Mater Letters 2006 859-863.
3. J. Zhu, A. Kamiya, T. Yamada, W. Shi, K. Naganuma; Mater Science and Eng A 2003 53-62.

4. S. Tamirisakandala, R.B. Bhat, J.S. Tiley, D.B. Miracle; Scripta Mater 2005 1421-1426.
5. B. Cherukuri, R. Srinivasan, S. Tamirisakandala, D.B. Miracle; Scripta Mater 2009 496-499.
6. W.J. Lu, R.J. Wu, D. Zhang, X.N. Zhang, T. Sakata, H. Mori; Comp Interfaces 2002 41-50.
7. D. Hill, R. Banerjee, D. Huber, J. Tiley, H.L. Fraser; Scripta Mater 2005 387-392.
8. T.T. Sasaki, B. Fu, K. Torres, G.B. Thompson, R. Srinivasan, J. Tiley; Phil Mag 2011 850-864.
9. P. Nandwana, S. Nag, D. Hill, J. Tiley, H.L. Fraser, R. Banerjee; Scripta Mater 2012 598-601.
10. H. Feng, Y. Zhou, D. Jia, Q. Meng, J. Rao; Crystal Growth & Design 2006 1626-1630.
11. W. Lu, D. Zhang, X. Zhang, R. Wu, T. Sakata, H. Mori; Journal of Alloys and Compounds 2001 240-247

Figure Caption

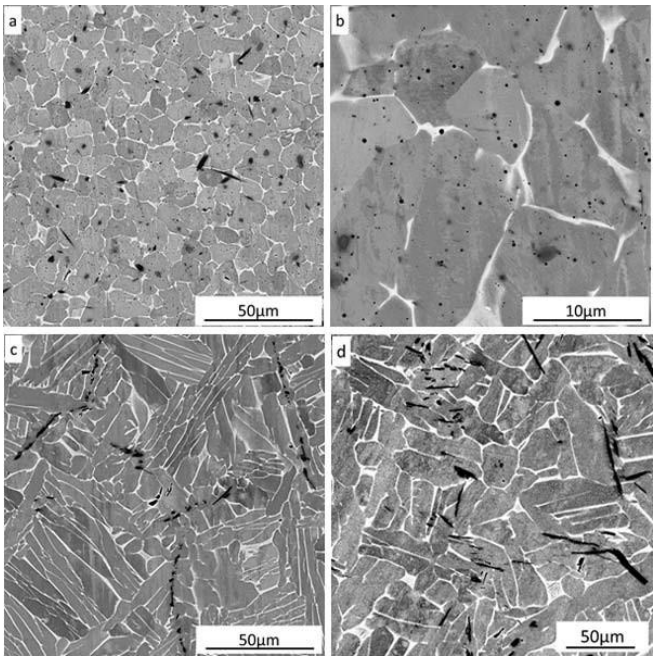

Fig. 1 Backscatter SEM images of SPS processed Ti64-1vol%TiB composite (a and b), arc melted Ti64-1vol%TiB composite (c) and arc-melted Ti64-2vol%TiB composite (d)

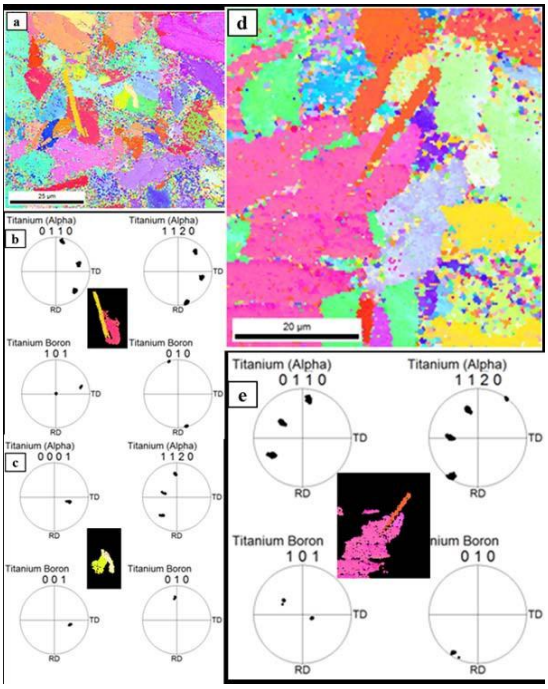

Fig. 2 (a) Inverse pole figure map of the overall microstructure of the SPS processed Ti64-1vol%TiB composite, (b) and (c) Highlighted regions consisting of selected boride precipitates and α precipitates and their corresponding pole figures, (d) Inverse pole figure map of a different region of the SPS processed Ti64-1vol%TiB composite and (e) Selected TiB and α precipitates with corresponding pole figures.

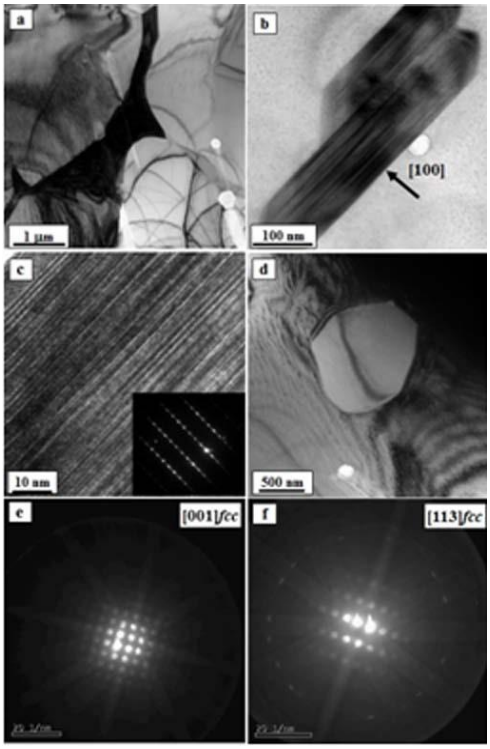

Fig. 3 (a) Bright field TEM image of the SPS processed 1.5 vol.%TiB/Ti-6Al-4V composite. (b) and (c) Higher magnification bright-field TEM images exhibiting a highly faulted TiB precipitate with faults parallel to $(100)_{TiB}$ planes viewed along the [001] zone axis (diffraction pattern shown as an inset). (d) Bright field TEM image of an equiaxed precipitate of the second titanium nitride phase present in the matrix. (e) and (f) Converged beam micro-diffraction patterns which can be consistently indexed as the [001] and [113] zone axes of titanium nitride, respectively.